Marine Chemistry 238 (2022) 104052

Contents lists available at ScienceDirect

Marine Chemistry

journal homepage: www.elsevier.com/locate/marchem

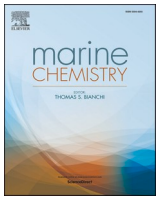

Spatial patterns and distributional controls of total and methylated mercury off the Lena River in the Laptev Sea sediments

Van Liem-Nguyen [a], Birgit Wild [a,b], Örjan Gustafsson [a,b], Igor Semiletov [c,d,e], Oleg Dudarev [c], Sofi Jonsson [a,*]

[a] Department of Environmental Science, Stockholm University, Sweden
[b] Bolin Centre for Climate Research, Stockholm University, Sweden
[c] Pacific Oceanological Institute, Russian Academy of Sciences, Vladivostok, Russia
[d] Department of Chemistry, Moscow State University, Moscow, Russia
[e] Centre for Arctic Land-Shelf System Research, Tomsk State University, Russia

A B S T R A C T

A warmer climate is predicted to accelerate the export of mercury (Hg) from Siberian rivers to the Arctic Ocean, yet there is a dearth of process-oriented studies on the speciation and fate of Hg in the shelf sea system. Here, we present data on total Hg (HgT) and methylmercury (MeHg) in Laptev Sea surface sediments along a cross-shelf transect starting at the mouth of the Lena River. Concentrations of HgT along the 330 km cross-shelf transect ranged within a fairly narrow span from 480 to 150 pmol g^{-1} d.w., while concentrations of MeHg decreased one hundredfold from 13 pmol g^{-1} d.w. near the Lena river to 0.095 pmol g^{-1} d.w. in the more distall stations. The highest concentrations of HgT and MeHg were observed close to the river delta and were associated with a high supply of organic carbon (OC). Enrichment of the OC normalized HgT concentration (HgT_{OC}) and depletion of the OC normalized MeHg concentration ($MeHg_{OC}$) across the shelf suggests bulk OC content to not be the only driver of the HgT and MeHg spatial distributions. Based on correlations observed between HgT_{OC} and $MeHg_{OC}$ and proxies for sediment physics and organic matter pools we suggest the spatial distribution of Hg and MeHg to also be influenced by hydrodynamic sorting of riverine-derived material. For MeHg, depletion of the $MeHg_{OC}$ across the shelf is likely driven by the trapping of terrestrial MeHg in sediments close to the river delta before it is degraded in the water column.

1. Introduction

The bioaccumulation and biomagnification of methylmercury (MeHg) in marine food webs becomes a globally recognized human health issue due to seafood consumption (Selin, 2009). The extent to which mercury (Hg) poses an environmental risk is governed by the complex biogeochemical cycle of Hg, including important land-ocean linkages. This is especially true for the Arctic Ocean, which accounts for only 1% of the global ocean volume, but receives more than 10% of the global river discharge (Shiklomanov, 1998). Furthermore, Arctic Ocean biogeochemistry is to a large extent influenced by benthic-pelagic couplings, as around half of the Arctic Ocean consists of shallow shelf areas. The East Siberian Arctic Shelf, covering the Laptev Sea, the East Siberian Sea, and the Russian part of the Chukchi Sea, is the largest continental shelf on earth and receives fluvial input from vast areas with continuous and discontinuous permafrost (Vonk et al., 2012). With the ongoing warming of the climate, many studies are now focusing on the vulnerability of the Siberian Arctic ecosystem, including the large stock of Hg stored in permafrost soils (7% of the global soil Hg pool contained in the upper 30 cm of permafrost according to estimates from Lim et al. (2020). Recent work demonstrates increased export of particulate mercury in Siberian rivers from areas with discontinuous or sporadic permafrost, in comparison to areas with continuous or no permafrost (Lim et al., 2019). Mu et al. (2019) further show Arctic riverine concentrations of total mercury (HgT) and MeHg to positively correlate with riverine discharge rates, and riverine discharge rates in turn to positively correlate with the average active layer thickness of the catchment area (the layer of the soil that undergoes seasonal thawing). Although coastal and shelf sediments can be presumed to act as a major receptor of terrestrial exports, they can at the same time be a source of MeHg to both benthic and pelagic ecosystems. Shelf sediments were, for example, recently suggested to be the main source of MeHg to the water-column of the East Siberian Sea (Kim et al., 2020).

The Lena River has the largest annual Hg flux (6600 kg yr^{-1}) of all Arctic rivers (Zolkos et al., 2020) and drains into the Laptev Sea, which covers an area of 498,000 km^2 and is the shallowest of the Arctic shelf seas with an average depth of only 48 m (Jakobsson et al., 2004; Weber, 1989). Organic carbon (OC) is the main vector for the transport of

* Corresponding author.
E-mail address: sofi.jonsson@aces.su.se (S. Jonsson).

https://doi.org/10.1016/j.marchem.2021.104052
Received 13 April 2021; Received in revised form 12 October 2021; Accepted 1 November 2021
Available online 12 November 2021

terrestrial Hg in riverine systems as well as for the accumulation of Hg in sediments (Zhang et al., 2015), and is thus highly relevant to discuss when investigating the land-ocean interactions of Hg. The main source of OC to Laptev Sea sediments is of terrestrial origin and derived from river runoff and coastal erosion of Pleistocene Ice Complex deposits (Bröder et al., 2019; Tesi et al., 2016; Vonk et al., 2012). The redistribution of terrestrial OC pools in the Laptev sea is suggested to be controlled by hydrodynamic sorting, with plant debris accumulating close to river deltas and mineral-bound fine fraction OC transported further out on the shelf (Tesi et al., 2016). Additionally, the terrestrial OC pool is subjected to cross-shelf degradation and dilution with marine-derived OC. As previously shown, these processes are reflected in surface sediments by e.g. a decreasing fraction of the OC occurring as lignin phenols (a terrestrial biomarker) and less depleted signals of $\delta^{13}C$ in the outer shelf (Bröder et al., 2016; Sparkes et al., 2016; Tesi et al., 2016; Tesi et al., 2014; Vonk et al., 2012). To what extent these processes also alter surface sediment concentrations of HgT and MeHg is, however, poorly known. Such information is vital to understand the effect permafrost thaw and increased transport of both OC and Hg by rivers will have on the environmental risk of Hg in the Arctic Ocean (i.e. the bioaccumulation of Hg in Arctic food webs).

Here, we provide data of HgT and MeHg concentrations over extensive offshore scales in Laptev Sea surface sediments. The study includes stations covering a Laptev Sea cross-shelf transect starting on the eastern side of the Lena River delta (an area that receives around 70% of the annual Lena River water discharge (Charkin et al., 2011, Semiletov et al., 2011)), as well as stations further east of the river delta that also receive material from the Lena river discharge (Fig. 1). The contrasting spatial distributions of bulk and OC-normalized HgT and MeHg concentrations were evaluated against sediment physical and organic matter properties.

2. Methods

2.1. Sampling information

Sediment samples were collected in August-September 2008 during the International Siberian Shelf Study 2008 (ISSS-08) expedition onboard the H/V Yacob Smirnitskyi (Archangelsk) and the smaller ship TB-0012 (Tiksi). The sampling activity was part of the International Polar Year (IPY) and the Arctic GEOTRACES programs. Surface sediment samples were collected with a Van Veen grab sampler as described elsewhere (Vonk et al., 2012). The samples were kept frozen during transport, freeze-dried and then stored dark at room temperature until further analysis.

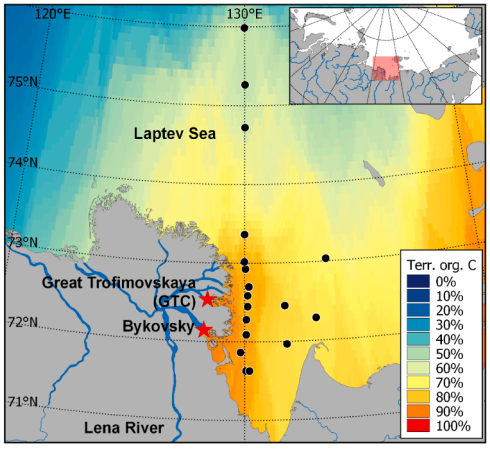

Fig. 1. Laptev Sea with sampling stations indicated with black circles and the fraction of terrestrial OC (estimated using ^{13}C data from (Martens et al., 2020)) indicated as the background color. Stars indicate the two main channels for the annual Lena River freshwater and sediment discharge, the Great Trofimovsakya Channels (GTC) and Bykovsky channels. The GTC and Bykovsky channel account for 60–75% and 20–25% of the water discharge entering the Buor-Kaya Bay, which is 80–90% of the annual Lena river discharge (Charkin et al., 2011; Semiletov et al., 2011).

2.2. Analytical measurements

Total Hg was measured using ~0.1 g of the freeze-dried sediment samples (weighted using a 5 digit scale) and a direct mercury analyzer (Milestone DMA-80, Italy). An in-house prepared reference material (a dried and homogenized sediment, 1.1 nmol Hg g^{-1}) was used for quality control. Observed HgT of this internal reference material was always within 96–101% of the previously determined HgT concentration.

For MeHg determination, 0.1 ml of 5.0 pmol g^{-1} $Me^{200}Hg$ enriched isotope (96.4%) and 0.9 ml Milli-Q water was added to 0.2–0.5 g of the sediments (weighted using a 5 digit scale) and then allowed to equilibrate for 1 h. After that, 2 ml of $CuSO_4$ (1 M), 10 ml KBr (1.4 M), and 10 ml CH_2Cl_2 were added to the samples. The MeHg in the sediment samples was extracted over 45 min while the samples were kept on an end-over-end rotator (30 rpm) (Lambertsson et al., 2001). The samples were then centrifuged (2 min, 1500 *g*) and the CH_2Cl_2 (lower layer) was transferred to a second test tube. The MeHg was then back-extracted into water by adding 10 ml of Milli-Q water to the CH_2Cl_2 and removing the CH_2Cl_2 by purging at 50 °C (N_2, 200 ml min^{-1}). The remaining water solution (about 10 ml) was transferred to a 40 ml brown glass vial with a septum, followed by the addition of 15 ml Milli-Q water, 225 µl acetate buffer (2 M, pH 5.0), and 30 µl sodium tetraethyl borate (STEB, 1%). The vial was vigorously shaken for 20 s and allowed to react for least 30 min before analysis. The analysis was conducted by coupling a methylmercury analyzer (Tekran 2700) with an inductively coupled plasma mass spectrometry (ICPMS, Thermo Scientific, XSeries 2). Concentrations of MeHg were then calculated from the internal standards as described elsewhere (Jonsson et al., 2012). Estuarine sediment certified material ERM-CC580 (74 ± 5 µg Hg g^{-1} as MeHg) was used for quality control. Determined concentrations of ERM-CC580 were within 96–102% of the certified MeHg concentration.

2.3. Sediment physical and organic carbon properties

The distribution of Hg is here evaluated in terms of sediment physical and organic carbon properties, which have been reported previously (Bröder et al., 2016; Sparkes et al., 2016; Tesi et al., 2016; Tesi et al., 2014; Vonk et al., 2012) and are summarized in Table S1. The fraction of terrestrial OC was calculated using average (± standard deviation) $\delta^{13}C$ end member signatures typical for this region of −23.2 ± 3.5 ‰ (marine) and − 26.7 ± 0.6 ‰ (terrestrial) (Martens et al., 2019). The terrestrial endmember assumes equal proportions of terrestrial OC from Ice Complex Deposits (ICD) ($\delta^{13}C$ signatures of −26.3 +/− 1 ‰; (Schirrmeister et al., 2011)) and active layer ($\delta^{13}C$ signatures of −27.1 +/− 0.7 ‰; (Martens et al., 2019)) sources. For TB-53 (a station close to the river delta), the fraction of terrestrial OC was set to 100% as the observed $\delta^{13}C$ signature (−27.5 ‰) was lower than that of the terrestrial endmember, but within the uncertainty range of active layer sources.

2.4. Statistics

All statistical treatment of the data was performed using the JMP® Pro (version 15.0.0) statistical software (SAS Institute Inc., Cary, NC, 1989–2019). The data-distribution of evaluated parameters was assessed using the Anderson-Darling test and visual inspection of density plots and Q-Q plots (Korkmaz et al., 2014). Log transformation of the parameters was applied when needed ($p > 0.05$) to obtain normal distribution prior to statistical analyses. Correlation analysis was done using linear regression on normally or log-normally distributed data (correlation coefficient, R^2, and correlation probability, p, reported). For

all statistical tests, significance was indicated by p (probability value) < 0.05. All concentrations are reported as per gram dry weight (d.w.).

3. Results and discussion

3.1. Spatial distribution of HgT and MeHg

We report surface sediment concentrations of HgT and MeHg from 18 stations in the Laptev Sea, covering a gradient of terrestrial organic matter input from the Lena river (Fig. 1). Concentrations of HgT and MeHg ranged from 150 to 480 pmol g^{-1} d.w. and 0.095 to 13 pmol g^{-1} d.w., respectively. These concentrations are within the ranges previously reported from other parts of the Arctic Ocean (Aksentov et al., 2021; Fox et al., 2014; Gobeil et al., 1999; Kim et al., 2020; Liu et al., 2015). In line with earlier work in other systems that identified OC as the main vector for Hg transport and accumulation in aquatic systems (Lambertsson and Nilsson, 2006; Zhao et al., 2019), the concentrations of HgT and MeHg correlated positively with OC content across all surface sediments (Fig. 2). The HgT_{OC}, ranging from 9.4 to 16 nmol g^{-1} in our study, is the same range as the HgT_{OC} recently reported from East Siberian Sea inner shelf sediments (10 to 20 nmol g^{-1} OC) (Aksentov et al., 2021).

Cross-shelf patterns of Hg were examined by expressing bulk and OC-normalized concentrations of HgT and MeHg (OC normalized concentrations hereafter referred to as HgT_{OC} and $MeHg_{OC}$, respectively) as a function of distance from the GTC (Figs. 1, 3 and S1), the main channel for the annual discharge of the Lena River (Charkin et al., 2011; Semiletov et al., 2011). Although the highest and the second-highest concentrations of HgT were observed in sediments close to the GTC (Table S1, Fig. 3), no significant correlation was found between bulk HgT concentrations and distance from the GTC (Fig. S1, $R^2 = 0.055$, $p = 0.35$). The HgT_{OC}, however, increased with distance from the GTC ($R^2 = 0.38$, $p = 0.0063$). Furthermore, decreasing concentrations of bulk MeHg and $MeHg_{OC}$ were observed with distance from the GTC ($R^2 = 0.44$, $p = 0.0028$ and $R^2 = 0.36$, $p = 0.0088$, respectively). These observations suggest bulk OC is not the only driver of the spatial distribution of HgT and MeHg on the shelf.

Previous characterization of the surface sediments analyzed here (Fig. 3, right column; Table S1) offers us the opportunity to further explore the distribution of Hg and MeHg as a function of sorting, degradation, and dilution of terrestrial OC on the shelf (Fig. 4, discussion below). Hydrodynamic sorting in combination with the degradation of the terrestrial OC during cross-shelf transport and dilution of terrestrial OC with marine substances results in decreasing bulk TOC and lignin phenol concentrations, increasing mineral specific surface area (SA), and more enriched $\delta^{13}C$ values with distance from the coast (Bröder et al., 2016; Sparkes et al., 2016; Tesi et al., 2016; Tesi et al., 2014; Vonk et al., 2012). These trends were also observed for the set of surface sediments included in this study (Fig. 3 and Fig. S1).

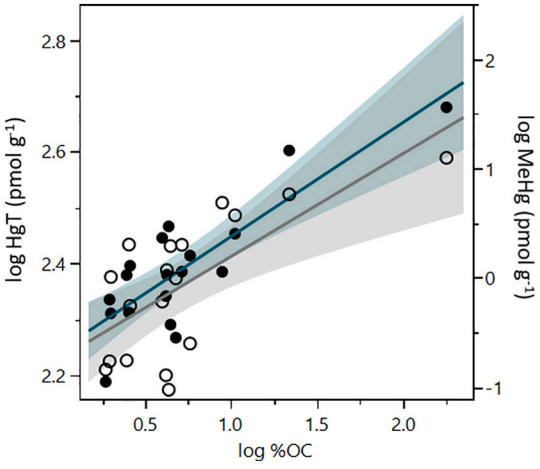

Fig. 2. Concentrations of HgT (filled circles, solid line) and MeHg (empty circles, broken line) as functions of OC content (%OC). Lines show the linear regression for HgT (solid line, $R^2 = 0.697$, $p < 0.0001$) and MeHg (broken line, $R^2 = 0.481$, $p = 0.0014$), and shaded area the 95% confidence of fit.

3.2. Processes controlling the spatial distribution of HgT

The spatial distribution of HgT was characterized by high concentrations at two of the stations located close to the GTC (400 and 480 pmol g^{-1}) and concentrations ranging from 150 to 280 pmol g^{-1} at the remaining stations. The two stations with the highest concentrations of HgT also had the highest concentrations of OC (38 and 95 mg g^{-1}) and the highest OC to SA ratios (3.2 and 6.9 mg m^{-2}). High OC to SA (exceeding 1 mg m^{-2}) is typically found in continental sediments receiving high loadings of OC (Mayer et al., 2002), suggesting the high concentration of HgT found to be driven by a high OC supply to these sediments. Although we observed a positive correlation between bulk HgT concentrations and the OC to SA ratio (Fig. 4, $R^2 = 0.5$, $p = 0.0023$) when testing the entire dataset, no significant correlation ($p = 0.79$) was found when removing the two stations with notably high OM and HgT concentrations (p = 0.79). Bulk concentration of HgT did not correlate with distance from the GTC, the fraction of terrestrial OC, lignin phenol concentration, nor with SA (Fig. 4). The lack of correlation between HgT and radioactive isotope $\Delta^{14}C$ signature (Fig. S1 and Table S1) further suggests that HgT does not depend on the age-related composition of the OC (i.e. OC deposited >10,000 yrs. ago and released from Ice Complex Deposits, hereon referred to as pre-aged OC, vs. more recently produced and exported OC from the terrestrial system or OC recently produced within the marine system). It should, however, be noted that the $\Delta^{14}C$ signatures observed at our stations, ranging from −310 to −560‰ (Table S1), suggest a significant accumulation of pre-aged permafrost OC in all our sediments (Bröder et al., 2016; Vonk et al., 2012). Overall, our observations suggest that, although high concentrations of HgT were found at stations with high OC supply, cross-shelf redistribution and dilution of the terrestrial OC pool do not control the spatial distribution of bulk HgT.

Although this was not the case for bulk concentrations of HgT, HgT_{OC} increased with distance from the GTC (Fig. 3 and Fig. S1). The concentrations of HgT_{OC} also correlated negatively with the fraction of terrestrial OC and the concentration of lignin phenols and positively with the SA (Fig. 4). Tesi et al. (2016) have demonstrated that particle properties (e.g. particle size and density) exert first-order control on the redistribution of terrestrial OC pools during cross-shelf transport in the Laptev and Eastern Siberian Sea Shelves. Close to the coast, plant debris is the main component of the bulk OC pool, while OC further out on the shelves is mainly associated with fine and ultrafine high-density particles. Lignin phenol concentrations are highest in plant fragments and are thus higher close to the coast where plant debris is retained due to hydrodynamic sorting. The correlation we observed between HgT_{OC} concentrations and the lignin phenol concentration and SA (low surface area indicating larger mineral particles) thus suggest hydrodynamic sorting of the terrestrial OC to also control the concentration of HgT_{OC}. Regional differences in the suspended matter HgT_{OC} have also been previously reported. Coquery et al. (1995) have, for example, reported suspended matter TOC and HgT concentrations corresponding to HgT_{OC} concentrations of 14 ± 12 and 46 nmol g^{-1} OC at stations located close to the Lena River delta and stations located in the area of our outermost stations, respectively. Although these observations represent snapshots of suspended matter HgT_{OC} at the time of sampling (September 1991), it is worth noting that they also observed higher HgT_{OC} in the area of the outermost stations. Furthermore, a recent study from the East Siberian Sea Aksentov et al. (2021) reports increasing HgT_{OC} (and HgT) with distance from the coast (1020 nmol Hg g^{-1} OC and 65 to 160 nmol Hg g^{-1} d.w. in the inner shelf (water depth of 0–50 m), 20–40 mmol Hg g^{-1}

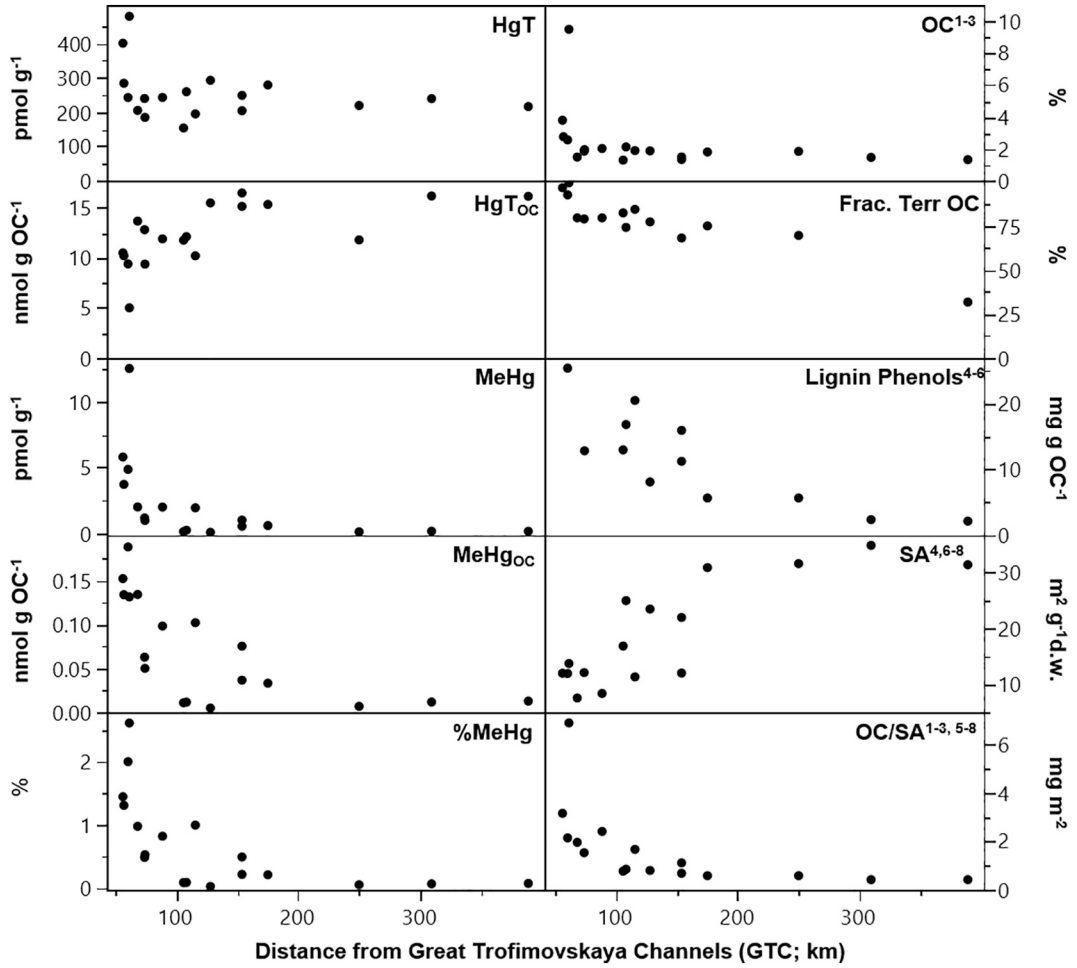

Fig. 3. Concentrations of HgT and MeHg (as bulk and OC-normalized concentrations) and %MeHg (of HgT) as a function of distance from the GTC (left column); concentrations of OC, fraction of terrestrial OC (Frac. Terr OC, calculated from ^{13}C signatures), lignin phenol concentration, mineral specific surface area (SA) and the OC to SA ratio as a function of distance from the GTC (right column). Data shown in the right column has previously been reported by Vonk et al. (2012), Sparkes et al. (2016), Tesi et al. (2016), Tesi et al. (2014), Bröder et al., 2016, Wennström R (2018), Karlsson et al. (2015) and Bröder et al. (2019).

OC and 220 to 350 nmol Hg g^{-1} d.w. in the outer shelf (water depth of 50–100 m)). These observations suggest that HgT_{OC} likely continues to increase with distance offshore and across the outer shelf of the Laptev Sea. The enrichment of Hg over OC along the transect may be a result of higher original HgT_{OC} content on the finer particles preferentially transported further out on the shelf, in comparison to the particles trapped close to the Lena River delta. The high affinity of Hg for finer sediments was previously suggested to account for the distribution of HgT as a result of hydrodynamic sorting processes in the central and southern Adriatic Sea sediments (Droghini et al., 2019) and in sediment from the Yangtze River estuarine-inner shelf of the East China Sea (Liu et al., 2017). In addition the more refractory nature of particles transported to the outer parts of the Laptev Sea shelf (Tesi et al., 2016) may prevent reduction and volatilization of particle-associated Hg and thus lead to higher ratios between Hg and OC in comparison to more nearshore stations (where most of the remineralization of terrestrial OC occurs (Bröder et al., 2016).

3.3. Processes controlling the spatial distribution of MeHg

Similar to HgT, the highest bulk concentrations of MeHg (5.8 and 13 pmol g^{-1}, Table S1) were found at the two stations closest to shore with high OC supplies (OC $\geq$ 38 mg g^{-1}), suggesting high OC load to also explain high MeHg bulk content. Across the shelf, however, the concentrations of MeHg in our surface sediments ranged over two orders of magnitudes, from 0.09 to 13 pmol g^{-1}, which is a much wider range than that of THg which varied by a factor of three (Fig. 3, Table S1). Accordingly, the fraction of HgT found as MeHg (%MeHg) decreases with distance from GTC by a factor of 40 (from 2.6% to 0.06%, Fig. 3 and Fig. S1). As MeHg is produced from inorganic Hg, the %MeHg is often used as a proxy for the 'net methylation' of Hg in natural environments (Liu et al., 2020; Tjerngren et al., 2012; Zhao et al., 2019). A positive correlation between the concentrations of HgT and MeHg was observed for our data (Fig. S2). Given the comparably stable concentrations of observed HgT, the spatial distribution of %MeHg therefore closely resembled the distribution of bulk MeHg (Fig. 3). Below, we thus discuss the spatial distribution of MeHg based on bulk MeHg and $MeHg_{OC}$ concentrations only (all trends discussed based on bulk MeHg and $MeHg_{OC}$ were, however, also true for %MeHg).

The higher MeHg and $MeHg_{OC}$ concentrations close to the GTC (Fig. 3, Table S1), and the sharp drop when moving away from the GTC, suggest high MeHg concentrations to be linked to terrestrial runoff. A similar decrease in the concentration of $MeHg_{OC}$ further suggests bulk OC content is not the only driver of the spatial distribution of MeHg. By evaluating the distribution of MeHg and $MeHg_{OC}$ against sediment physical and organic matter properties (Fig. 4), we here explore the potential role of i) dilution of the terrestrial OC pool with marine-derived OC and ii) hydrodynamic sorting processes for the spatial distribution of MeHg. Using the average ($\pm$ standard deviation) $\delta^{13}C$ signatures of -23.2 ± 3.5‰ and -26.7 ± 0.6 ‰ for the marine and

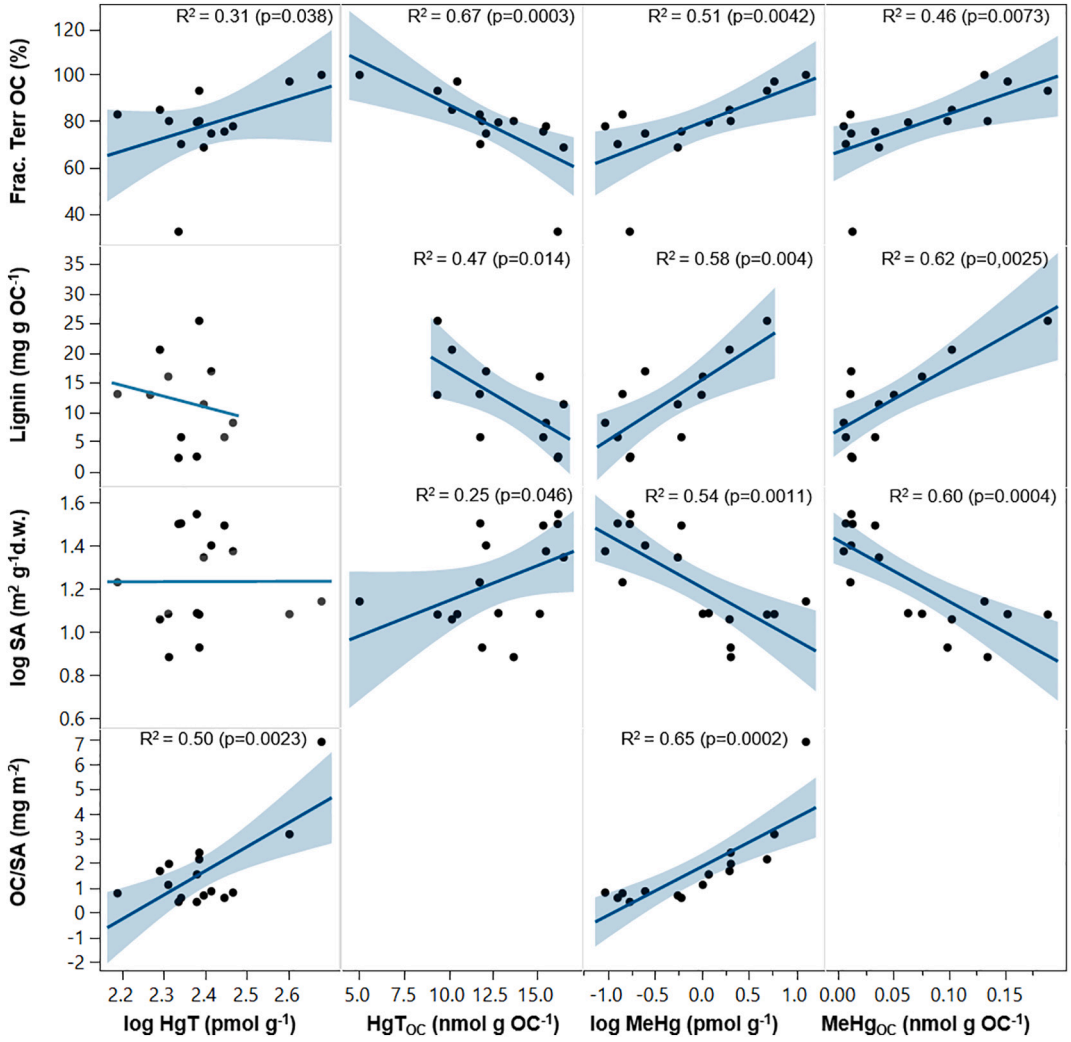

Fig. 4. Correlation between (on the x-axis) HgT, HgT_{OC} (HgT/OC ratio), MeHg, and MeHgOC and (on the y-axis) fraction of terrestrial OC (Frac. Terr OC), concentration of lignin phenols, mineral specific surface area (SA) and the OC to SA ratio. Lines shows the linear regression for and shaded area the 95% confidence of fit for correlations where $p < 0.05$, R^2 and F test result given in each graph.

terrestrial endmembers (Martens et al., 2019; Schirrmeister et al., 2011), respectively, the fraction of terrestrial OC was calculated to range from 68 to 100%, with the exception of the outermost station where only 32% of the OC was of terrestrial origin (Fig. 3, Table S1). To test if dilution of the terrestrial OC pool could explain the spatial distribution of MeHg observed, we predicted the bulk concentration of MeHg associated with the terrestrial OC pool using the calculated bulk terrestrial OC concentration and by assuming a constant $MeHg_{OC}$ for the terrestrial OC pool at all stations (Fig. S3). For stations with a fraction of terrestrial OC below 80%, the predicted bulk MeHg concentration (associated with the terrestrial OC pool) on average exceeded the observed concentrations of MeHg by an order of magnitude. These results suggest that dilution of the terrestrial OC pool with marine derived OC alone did not explain the spatial distribution of MeHg. It is more likely that hydrodynamic sorting alters the distribution of $MeHg_{OC}$, as suggested by the correlation found between $MeHg_{OC}$ and concentrations of lignin phenols as well as SA (Fig. 4). We further note that a correlation was observed between MeHg concentrations and the OC to SA ratio. The ratio between OC and SA in sediments can be used to estimate oxygen exposure times, where a low ratio indicates long oxygen exposure time. Bröder et al. (2016) have previously shown that high OC to SA ratios close to the Lena River delta dropped sharply with distance from the offshore, suggesting extensive remineralization of the OC close to the coast. Similarly, MeHg dropped over a relatively short spatial scale (Fig. 3), and the bulk concentration of MeHg correlated positively with the OC to SA ratio (even when the two stations with notably high OC loadings were removed). It is reasonable to assume that remineralization of OC also results in the degradation of terrestrially derived MeHg. Remineralization of OC may lead to more MeHg becoming available for photochemically and microbially mediated demethylation processes (Bowman et al., 2020; DiMento and Mason, 2017; Marvin-DiPasquale et al., 2000) by releasing it from the particulate matter or by promoting demethylation through the production of dissolved OC, which may enhance photochemical demethylation rates (Zhang and Hsu-Kim, 2010). The degradation of MeHg could also be directly linked to remineralization processes. Organomercury lyase (MerB), an operon encoding for microbial demethylation of MeHg, has e.g. recently been identified in Arctic waters (Bowman et al., 2020), suggesting that microorganisms carrying this operon could play a role. The MerB has also been found in other compartments in the arctic including permafrost soils (Mindlin et al., 2005). Furthermore, some methanotrophs have been shown to rapidly take up and degrade MeHg in laboratory experiments (Lu et al., 2017).

In addition to terrestrial loading of MeHg, MeHg can be produced in sediment and marine waters through microbial methylation of inorganic Hg (Kirk et al., 2008; Lehnherr et al., 2011). Work by Kim et al. (2020), however, suggests water column Hg methylation to be an unlikely driver of shelf sediment MeHg concentrations. Instead, their mass budget of MeHg in the East Siberian Sea shelf suggests sediment to act as a source

of MeHg to the water column and the flux of MeHg from shelf sediment to be two orders of magnitude greater than water column gross Hg methylation. Although this mass budget does not cover the Laptev Sea, water column Hg methylation in Laptev Sea shelf waters is most likely limited, in comparison to the East Siberian Sea, given the higher biological productivity in the East Siberian Sea due to the inputs of nutrient-rich Pacific waters (Popova et al., 2010; Walsh et al., 1989). Extensive net methylation of Hg as the riverine particles are transported in the coastal area, as previously shown in other systems (Capo et al., 2020; Ortiz et al., 2015) is also unlikely to explain observed MeHg trends, as we would then expect higher concentrations of MeHg further off the coast, where more remineralized OC settles. We cannot entirely exclude the contribution from potentially higher in situ production of MeHg in sediments close to the GTC due to the higher fraction of degradable OC. We note, however, that MeHg concentration does not correlate with the degradable fine fraction of OC previously reported by Bröder et al. (2019) (Fig. S4). The abundance of terrestrial DOM (which is less available to microbes) further makes significant in situ production of MeHg in these sediments less likely (Bravo et al., 2017). Over what timeframes MeHg deposited or produced in situ may persist in surface sediments is currently not well known. Earlier studies, however, suggest a significant fraction of the MeHg in sediments to be refractory (i.e., not readily available for demethylation), at least over the timeframe of weeks to months (Girard et al., 2016; Jonsson et al., 2014; Liem-Nguyen et al., 2016). These earlier observations support that riverine sources of MeHg can accumulate over time in coastal sediments where sediment accumulation rates are relatively high. Regardless of whether or not in situ methylation contributes to the higher MeHg concentrations observed close to the GTC, our data support hydrodynamic sorting to be a key determinant of the spatial distribution of MeHg off the Lena River on the Laptev Sea. This could either be by trapping terrestrially derived MeHg in sediments close to the river delta before the MeHg has time to degrade in the water column, or by fueling in situ sedimentary MeHg production through trapping of the less degraded OC close to the coast.

3.4. Conclusions

Here we show that the accumulation of HgT-rich material closest to the Lena River delta is associated with high accumulation of terrestrial material rich in OC. Further out on the shelf, however, we suggest that sorting of the terrestrial OC leads to enriched concentrations of HgT relative to the bulk OC content. Also for MeHg, hydrodynamic sorting was demonstrated to play a key role in its distribution within the investigated area, with higher concentrations of MeHg accumulating closer to the river delta. Across our stations, THg varied by a factor of three while the concentrations of MeHg in our surface sediments ranged over two orders of magnitudes, suggesting that hydrodynamic sorting exerts greater control on the distribution of MeHg than HgT.

Previous studies have highlighted a greater availability of recent MeHg loadings for bioaccumulation into benthic invertebrates in a coastal system in comparison to MeHg buried a few mm below the sediment surface (Jonsson et al., 2017; Jonsson et al., 2014). The amount of MeHg accumulated in benthic communities, and transferred via benthic-pelagic food web coupling to higher organisms, can thus be expected to quickly respond to altered concentrations of MeHg in surface sediments. The higher MeHg concentrations observed near the river delta, suggest that coastal food webs in this area are more vulnerable to terrestrial loadings of MeHg than benthic communities further out on the shelf. Inputs of both HgT (mainly consisting of inorganic Hg) and MeHg are predicted to increase with accelerated riverine discharge rates and permafrost degradation (Mu et al., 2019). As a result of greater sedimentation rates close to the delta, and faster delivery of terrestrial MeHg further off the coast, the area with higher MeHg concentrations in the surface sediments will likely expand. Our study demonstrates the need to better understand benthic-pelagic coupling in the area of the river delta to better comprehend the risk of future terrestrial MeHg loadings to the Siberian Arctic Shelf areas.

Declaration of Competing Interest

None.

Acknowledgment

This research was supported by the European Research Council (ERC Advanced Grant CC-TOP 392 695331 to ÖG), and the Swedish Research Council (Grant 2017-01601). Field campaigns were supported by the Knut and Alice Wallenberg Foundation (KAW contract 2011.0027 to ÖG) as well as by the Russian Government (grant 14, Z50.31.0012 to IS). We thank the crew and personnel of the R/V Academician M. Keldish. Igor Semiletov and Oleg V. Dudarev acknowledges the Russian Scientific Foundation (grant no. 21-77-30001 to IS)

Appendix A. Supplementary data

Supplementary data to this article can be found online at https://doi.org/10.1016/j.marchem.2021.104052.

References

Aksentov, K.I., Astakhov, A.S., Ivanov, M.V., Shi, X., Hu, L., Alatortsev, A.V., Sattarova, V.V., Mariash, A.A., Melgunov, M.S., 2021. Assessment of mercury levels in modern sediments of the east Siberian Sea. Mar. Pollut. Bull. 168, 112426.

Bowman, K.L., Collins, R.E., Agather, A.M., Lamborg, C.H., Hammerschmidt, C.R., Kaul, D., Dupont, C.L., Christensen, G.A., Elias, D.A., 2020. Distribution of mercury-cycling genes in the Arctic and equatorial Pacific oceans and their relationship to mercury speciation. Limnol. Oceanogr. 65, S310–S320.

Bravo, A.G., Bouchet, S., Tolu, J., Björn, E., Mateos-Rivera, A., Bertilsson, S., 2017. Molecular composition of organic matter controls methylmercury formation in boreal lakes. Nat. Commun. 8, 14255.

Bröder, L., Tesi, T., Salvadó, J.A., Semiletov, I.P., Dudarev, O.V., Gustafsson, Ö., 2016. Fate of terrigenous organic matter across the Laptev Sea from the mouth of the Lena River to the deep sea of the Arctic interior. Biogeosciences 13 (17), 5003–5019.

Bröder, L., Andersson, A., Tesi, T., Semiletov, I., Gustafsson, Ö., 2019. Quantifying degradative loss of terrigenous organic carbon in surface sediments across the Laptev and east Siberian Sea. Glob. Biogeochem. Cycles 33 (1), 85–99.

Capo, E., Bravo, A.G., Soerensen, A.L., Bertilsson, S., Pinhassi, J., Feng, C., Andersson, A. F., Buck, M., Björn, E., 2020. Deltaproteobacteria and Spirochaetes-Like Bacteria Are Abundant Putative Mercury Methylators in Oxygen-Deficient Water and Marine Particles in the Baltic Sea. Frontiers in Microbiology 11, 574080. https://doi.org/10.3389/fmicb.2020.574080.

Charkin, A.N., Dudarev, O.V., Semiletov, I.P., Kruhmalev, A., Vonk, J., Sánchez-García, L., Karlsson, E., Gustafsson, Ö., 2011. Seasonal and interannual variability of sedimentation and organic matter distribution in the Buor-Khaya gulf: the primary recipient of input from Lena River and coastal erosion in the Southeast Laptev Sea. Biogeosciences 8 (9), 2581–2594.

Coquery, M., Cossa, D., Martin, J., 1995. The distribution of dissolved and particulate mercury in three Siberian estuaries and adjacent Arctic coastal waters. Water Air Soil Pollut. 80 (1–4), 653–664.

DiMento, B.P., Mason, R.P., 2017. Factors controlling the photochemical degradation of methylmercury in coastal and oceanic waters. Mar. Chem. 196, 116–125.

Droghini, E., Annibaldi, A., Prezioso, E., Tramontana, M., Frapiccini, E., De Marco, R., Illuminati, S., Truzzi, C., Spagnoli, F., 2019. Mercury content in central and southern Adriatic Sea sediments in relation to seafloor geochemistry and sedimentology. Molecules 24 (24), 4467.

Fox, A.L., Hughes, E.A., Trocine, R.P., Trefry, J.H., Schonberg, S.V., McTigue, N.D., Lasorsa, B.K., Konar, B., Cooper, L.W., 2014. Mercury in the northeastern Chukchi Sea: distribution patterns in seawater and sediments and biomagnification in the benthic food web. Deep-Sea Res. II Top. Stud. Oceanogr. 102, 56–67.

Girard, C., Leclerc, M., Amyot, M., 2016. Photodemethylation of methylmercury in eastern Canadian Arctic thaw pond and lake ecosystems. Environ. Sci. Technol. 50 (7), 3511–3520.

Gobeil, C., Macdonald, R.W., Smith, J.N., 1999. Mercury profiles in sediments of the Arctic Ocean basins. Environ. Sci. Technol. 33 (23), 4194–4198.

Jakobsson, M., Grantz, A., Kristoffersen, Y., Macnab, R., 2004. In: Stein, R., Macdonald, R.W. (Eds.), The Organic Carbon Cycle in the Arctic Ocean. Springer, Berlin.

Jonsson, S., Skyllberg, U., Nilsson, M.B., Westlund, P.-O., Shchukarev, A., Lundberg, E., Björn, E., 2012. Mercury methylation rates for geochemically relevant HgII species in sediments. Environ. Sci. Technol. 46 (21), 11653–11659.

Jonsson, S., Skyllberg, U., Nilsson, M.B., Lundberg, E., Andersson, A., Björn, E., 2014. Differentiated availability of geochemical mercury pools controls methylmercury levels in estuarine sediment and biota. Nat. Commun. 5.

Jonsson, S., Andersson, A., Nilsson, M.B., Skyllberg, U., Lundberg, E., Schaefer, J.K., Åkerblom, S., Björn, E., 2017. Terrestrial discharges mediate trophic shifts and enhance methylmercury accumulation in estuarine biota. Sci. Adv. 3 (1), e1601239.
Karlsson, E.S., Brüchert, V., Tesi, T., Charkin, A., Dudarev, O., Semiletov, I., Gustafsson, Ö., 2015. Contrasting regimes for organic matter degradation in the East Siberian Sea and the Laptev Sea assessed through microbial incubations and molecular markers. Mar. Chem. 170, 11–22.
Kim, J., Soerensen, A.L., Kim, M.S., Eom, S., Rhee, T.S., Jin, Y.K., Han, S., 2020. Mass budget of methylmercury in the east Siberian Sea: the importance of sediment sources. Environ. Sci. Technol. 54 (16), 9949–9957.
Kirk, J.L., St Louis, V.L., Hintelmann, H., Lehnherr, I., Else, B., Poissant, L., 2008. Methylated mercury species in marine waters of the Canadian high and sub Arctic. Environ. Sci. Technol. 42 (22), 8367–8373.
Korkmaz, S., Goksuluk, D., Zararsiz, G., 2014. MVN: an R package for assessing multivariate normality. R J. 6 (2), 151–162.
Lambertsson, L., Nilsson, M., 2006. Organic material: the primary control on mercury methylation and ambient methyl mercury concentrations in estuarine sediments. Environ. Sci. Technol. 40 (6), 1822–1829.
Lambertsson, L., Lundberg, E., Nilsson, M., Frech, W., 2001. Applications of enriched stable isotope tracers in combination with isotope dilution GC-ICP-MS to study mercury species transformation in sea sediments during in situ ethylation and determination. J. Anal. At. Spectrom. 16 (11), 1296–1301.
Lehnherr, I., Louis, V.L.S., Hintelmann, H., Kirk, J.L., 2011. Methylation of inorganic mercury in polar marine waters. Nat. Geosci. 4 (5), 298.
Liem-Nguyen, V., Jonsson, S., Skyllberg, U., Nilsson, M.B., Andersson, A., Lundberg, E., Björn, E., 2016. Effects of nutrient loading and mercury chemical speciation on the formation and degradation of methylmercury in estuarine sediment. Environ. Sci. Technol. 50 (13), 6983–6990.
Lim, A.G., Sonke, J.E., Krickov, I.V., Manasypov, R.M., Loiko, S.V., Pokrovsky, O.S., 2019. Enhanced particulate hg export at the permafrost boundary, western Siberia. Environ. Pollut. 254, 113083.
Lim, A.G., Jiskra, M., Sonke, J.E., Loiko, S.V., Kosykh, N., Pokrovsky, O.S., 2020. A revised pan-Arctic permafrost soil Hg pool based on Western Siberian peat Hg and carbon observations. Biogeosciences 17 (12), 3083–3097.
Liu, Y., Chai, X., Hao, Y., Gao, X., Lu, Z., Zhao, Y., Zhang, J., Cai, M., 2015. Total mercury and methylmercury distributions in surface sediments from Kongsfjorden, Svalbard, Norwegian Arctic. Environ. Sci. Pollut. Res. 22 (11), 8603–8610.
Liu, W., Hu, L., Lin, T., Li, Y., Guo, Z., 2017. Distribution and mass inventory of mercury in sediment from the Yangtze River estuarine-inner shelf of the East China Sea. Cont. Shelf Res. 132, 29–37.
Liu, J., Wang, D., Zhang, J., Liem-Nguyen, V., Huang, R., Jiang, T., 2020. Evaluation of Hg methylation in the water-level-fluctuation zone of the three gorges reservoir region by using the MeHg/HgT ratio. Ecotoxicol. Environ. Saf. 195, 110468.
Lu, X., Gu, W., Zhao, L., Haque, M.F.U., DiSpirito, A.A., Semrau, J.D., Gu, B., 2017. Methylmercury uptake and degradation by methanotrophs. Sci. Adv. 3 (5), e1700041.
Martens, J., Wild, B., Pearce, C., Tesi, T., Andersson, A., Bröder, L., O'Regan, M., Jakobsson, M., Sköld, M., Gemery, L., 2019. Remobilization of old permafrost carbon to Chukchi Sea sediments during the end of the last deglaciation. Glob. Biogeochem. Cycles 33 (1), 2–14.
Martens, J., Romankevich, E., Semiletov, I., Wild, B., van Dongen, B., Vonk, J., Tesi, T., Shakhova, N., Dudarev, O.V., Kosmach, D., 2020. CASCADE–the Circum-Arctic sediment CArbon databasE. Earth Syst. Sci. Data Discus. 1–26.
Marvin-DiPasquale, M., Agee, J., McGowan, C., Oremland, R.S., Thomas, M., Krabbenhoft, D., Gilmour, C.C., 2000. Methyl-mercury degradation pathways: a comparison among three mercury-impacted ecosystems. Environ. Sci. Technol. 34 (23), 4908–4916.
Mayer, L., Benninger, L., Bock, M., DeMaster, D., Roberts, Q., Martens, C., 2002. Mineral associations and nutritional quality of organic matter in shelf and upper slope sediments off Cape Hatteras, USA: a case of unusually high loadings. Deep-Sea Res. II Top. Stud. Oceanogr. 49 (20), 4587–4597.
Mindlin, S., Minakhin, L., Petrova, M., Kholodii, G., Minakhina, S., Gorlenko, Z., Nikiforov, V., 2005. Present-day mercury resistance transposons are common in bacteria preserved in permafrost grounds since the upper Pleistocene. Res. Microbiol. 156 (10), 994–1004.
Mu, C., Zhang, F., Chen, X., Ge, S., Mu, M., Jia, L., Wu, Q., Zhang, T., 2019. Carbon and mercury export from the Arctic rivers and response to permafrost degradation. Water Res. 161, 54–60.
Ortiz, V.L., Mason, R.P., Ward, J.E., 2015. An examination of the factors influencing mercury and methylmercury particulate distributions, methylation and demethylation rates in laboratory-generated marine snow. Mar. Chem. 177, 753–762.
Popova, E., Yool, A., Coward, A., Aksenov, Y., Alderson, S., De Cuevas, B., Anderson, T., 2010. Control of primary production in the Arctic by nutrients and light: insights from a high resolution ocean general circulation model. Biogeosciences 7 (11), 3569–3591.
Schirrmeister, L., Kunitsky, V., Grosse, G., Wetterich, S., Meyer, H., Schwamborn, G., Babiy, O., Derevyagin, A., Siegert, C., 2011. Sedimentary characteristics and origin of the late pleistocene ice complex on north-east Siberian Arctic coastal lowlands and islands–a review. Quat. Int. 241 (1–2), 3–25.
Selin, N.E., 2009. Global biogeochemical cycling of mercury: a review. Annu. Rev. Environ. Resour. 34.
Semiletov, I.P., Pipko, I.I., Shakhova, N.E., Dudarev, O.V., Pugach, S.P., Charkin, A.N., McRoy, C., Kosmach, D., Gustafsson, Ö., 2011. Carbon transport by the Lena River from its headwaters to the Arctic Ocean, with emphasis on fluvial input of terrestrial particulate organic carbon vs. carbon transport by coastal erosion. Biogeosciences 8 (9), 2407–2426.
Shiklomanov, I., 1998. A New Appraisal and Assessment for the 21st Century. World Water Resources.
Sparkes, R.B., Dogrul Selver, A., Gustafsson, Ö., Semiletov, I.P., Haghipour, N., Wacker, L., Eglinton, T.I., Talbot, H.M., Van Dongen, B.E., 2016. Macromolecular composition of terrestrial and marine organic matter in sediments across the east Siberian Arctic shelf. The Cryosphere 10 (5), 2485–2500.
Tesi, T., Semiletov, I., Hugelius, G., Dudarev, O., Kuhry, P., Gustafsson, Ö., 2014. Composition and fate of terrigenous organic matter along the Arctic land–ocean continuum in East Siberia: insights from biomarkers and carbon isotopes. Geochim. Cosmochim. Acta 133, 235–256.
Tesi, T., Semiletov, I., Dudarev, O., Andersson, A., Gustafsson, Ö., 2016. Matrix association effects on hydrodynamic sorting and degradation of terrestrial organic matter during cross-shelf transport in the Laptev and east Siberian shelf seas. J. Geophys. Res. Biogeosci. 121 (3), 731–752.
Tjerngren, I., Meili, M., Björn, E., Skyllberg, U., 2012. Eight boreal wetlands as sources and sinks for methyl mercury in relation to soil acidity, C/N ratio, and small-scale flooding. Environ. Sci. Technol. 46 (15), 8052–8060.
Vonk, J.E., Sánchez-García, L., Van Dongen, B., Alling, V., Kosmach, D., Charkin, A., Semiletov, I.P., Dudarev, O.V., Shakhova, N., Roos, P., 2012. Activation of old carbon by erosion of coastal and subsea permafrost in Arctic Siberia. Nature 489 (7414), 137.
Walsh, J.J., McRoy, C., Coachman, L., Goering, J., Nihoul, J., Whitledge, T., Blackburn, T., Parker, P., Wirick, C., Shuert, P., 1989. Carbon and nitrogen cycling within the Bering/Chukchi seas: source regions for organic matter effecting AOU demands of the Arctic Ocean. Prog. Oceanogr. 22 (4), 277–359.
Weber, J., 1989. The Arctic Seas. Springer, pp. 797–828.
Zhang, T., Hsu-Kim, H., 2010. Photolytic degradation of methylmercury enhanced by binding to natural organic ligands. Nat. Geosci. 3 (7), 473–476.
Zhang, Y., Jacob, D.J., Dutkiewicz, S., Amos, H.M., Long, M.S., Sunderland, E.M., 2015. Biogeochemical drivers of the fate of riverine mercury discharged to the global and Arctic oceans. Glob. Biogeochem. Cycles 29 (6), 854–864.
Zhao, L., Wang, R., Zhang, C., Yin, D., Yang, S., Huang, X., 2019. Geochemical controls on the distribution of mercury and methylmercury in sediments of the coastal East China Sea. Sci. Total Environ. 667, 133–141.
Zolkos, S., Krabbenhoft, D.P., Suslova, A., Tank, S.E., McClelland, J.W., Spencer, R.G., Shiklomanov, A., Zhulidov, A.V., Gurtovaya, T., Zimov, N., 2020. Mercury export from Arctic great Rivers. Environ. Sci. Technol. 54 (7), 4140–4148.